From cartoons to quantitative models in Golgi transport

D. Nicolas Quiros[1,2], Franco Nieto[1] and Luis S. Mayorga[1,2,*]

[1]IHEM (Universidad Nacional de Cuyo, CONICET), [2]Facultad de Ciencias Exactas y Naturales, Mendoza, Argentina.

[*]Correspondence:

Luis S. Mayorga

Phone: 54 261 4054843

lmayorga@fcm.uncu.edu.ar or lmayorga@mendoza-conicet.gob.ar

Running title: **Golgi transport models**

Keywords: intracellular trafficking, Golgi transport, quantitative cell biology, Agent-based models, Repast, COPASI

Abbreviations:

ABM, agent-based model; ER, endoplasmic reticulum; ERGIC, endoplasmic reticulum Golgi intermediate compartment; ODE, ordinary differential equations; TGN, Trans Golgi Network

Acknowledgments:

The authors would like to thank G. Flores for help in the programming of the model and A. Luini, S. Parashuraman, and G. Sager for helpful discussions.

Funding:

This work was supported in part by grants from Universidad Nacional de Cuyo (Mendoza, Argentina) [06/M116] and Agencia Nacional de Promoción Científica y Tecnológica (Argentina) [PICT-2016-0894, PICT 2018-4451] to L.S.M. F.N. obainded a fellowship from Consejo Nacional de Investigaciones Científicas y Técnicas (Argentina). LSM was supported by CONICET (Consejo Nacional de Investigaciones Científicas y Técnicas, Argentina).

Author contribution:

LSM: concept and design of the research, data analysis, and interpretation, wrote of the article; DNQ and FN: run simulations, data analysis, and interpretation.

Abstract

Background. Cell biology is evolving to become a more formal and quantitative science. In particular, several mathematical models have been proposed to address Golgi self-organization and protein and lipid transport. However, most scientific articles about the Golgi apparatus are still using static cartoons that miss the dynamism of this organelle.

Results. In this report, we show that schematic drawings of Golgi trafficking can be easily translated into an Agent-Based Model using the Repast platform. The simulations generate an active interplay among cisternae and vesicles rendering quantitative predictions about Golgi stability and transport of soluble and membrane-associated cargoes. The models can incorporate complex networks of molecular interactions and chemical reactions by association with COPASI, a software that handles Ordinary Differential Equations.

Conclusions. The strategy described provides a simple, flexible, and multiscale support to analyze Golgi transport. The simulations can be used to address issues directly linked to the mechanism of transport or as a way to incorporate the complexity of trafficking to other cellular processes that occur in dynamic organelles.

Significance. We show that the rules implicitly present in most schematic representations of intracellular trafficking can be used to build dynamic models with quantitative outputs that can be compared with experimental results.

Introduction

Intracellular trafficking is a fundamental process for eukaryotic cells. Macromolecules need to find their way along the endocytic and secretory pathways to their final destination in the interior of the cell or to be secreted to the extracellular medium. It is not easy to envision this active exchange of material between membrane-bound structures. As a rule, macromolecules do not leave the donor organelle to travel through the cytoplasm to be incorporated into the acceptor compartment. Hence, transport requires the interaction and exchange of soluble and membrane-associated components among closed compartments. Whether the exchange is direct between the compartments or mediated by tubulo-vesicular transport carriers, the process requires two opposite and complementary events. Membrane fusion that allows the mixing of two organelles, and membrane fission that mediates the segregation and sorting of molecules among the dividing structures.

The mechanism of membrane fusion has been studied in detail (Wickner and Schekman, 2008; Sudhof and Rothman, 2009; Jahn and Fasshauer, 2012). A central core of proteins is required for membrane apposition and bilayer destabilization to promote the opening and expansion of a fusion pore connecting the membrane-bound structures. Besides the protein complex required to overcome the energetic barrier involved in the formation of the pore, another set of proteins are needed to provide specificity to the process. Fusion must occur among compatible organelles to preserve the complex organization of the cell. As a rule, organelles surrounded by similar membrane domains have a higher probability of fusing.

Membrane fission is also a well-characterized process (Renard et al., 2018). Depending on their protein and lipid composition, different membrane domains bind membrane-deforming protein complexes, such as COPs, clathrin, sorting nexins, and others (Bonifacino and Glick, 2004) (McCullough et al., 2013). The deformations lead to the sorting of membrane domains by budding of tubules or vesicles that are now separated from the original organelle.

Upon fusion, membrane domains do not necessarily mix. It is well recognized the presence of separate membrane domains within a single organelle (Miaczynska and Zerial, 2002). Membrane domains can then be considered as key building blocks of the cellular endomembrane system, and they have special characteristics for each subcellular compartment. Membrane domains are not static, and can dynamically change their composition. In this scenario, soluble and membrane-

bound cargoes are directed to their final destination following the fusion/fission interplay among organelles. The terminal location of a molecule depends on its behavior during these events. Soluble cargoes that do not interact with membranes are transported in the lumen of the organelles; hence, during fission, they are distributed according to the volume of the newly formed organelles. Fluid-phase cargoes are enriched in round, large-volume structures and excluded from small vesicles and tubules. Membrane cargoes with no particular affinity for a membrane domain, similar to soluble cargoes, are distributed proportionally to the area of organelles. However, membrane cargoes frequently carry specific tags that interact with one or more adaptor proteins that strongly affect their destination during fission (Kim, 2016). In addition, lipids in membranes are organized in microdomains, and membrane-anchored factors are also recruited to specific lipid environments that are segregated during the formation of vesicles and tubules (Kumar et al., 2015).

Despite the detailed knowledge about the molecular mechanisms involved in transport and the large list of factors that have been identified, the underlying logic of the process is still not well understood. For example, a classical controversy between vesicular transport and maturation in Golgi transport is still present after several decades and hundreds of experiments using very ingenious tools to discriminate between the two models. Interestingly, both are presented as possibilities in Cell Biology books (Alberts et al., 2015), reviews (Glick and Luini, 2011), and encyclopedias (Luini and Parashuraman, 2016). At present, the evidence points to maturation as the main transport mechanism (Glick and Luini, 2011). In yeast, where the Golgi is not organized in stacks, the maturation of a single cisterna containing a fluorescent cargo has been observed in real-time images (Kurokawa et al., 2019). Besides, mathematical modeling (Mani and Thattai, 2016) and experimental data about the mechanism of transport of Golgi resident proteins are consistent with maturation (Liu et al., 2018).

Part of the problem is that hypotheses in intracellular transport are in general qualitative, like most postulates in Cell Biology. They are presented as schematic representations of compartments connected by arrows and seldom translated to formal models with quantitative predictions. The dynamic nature of organelles that change position, shape, and composition makes it difficult to develop simple formal models for intracellular transport. Our group has shown that modeling of a simplified endocytic route composed of early, sorting, recycling, and late endosomes is possible using two complementary techniques: i) Agent-Based Modeling (ABM) to handle movement, fusion, and fission of organelles, and ii) Ordinary Differential Equations (ODE), to deal with molecule interactions and chemical reactions. Simulations generated with this model accurately reproduce several experimental results and could be used as a platform to represent complex molecular events such as Rab conversion, endosomal acidification, transport of lysosomal enzymes, and hydrolysis of glycolipids (Mayorga et al., 2018).

The flexibility of ABM allows building simulations with quantitative outputs from schematic representations of biological processes. An agent can be anything from a single molecule to a complete organelle. The behavior of the agents can be specified with simple rules that parallel the

way of thinking in informal models. For example, the fusion among two organelles can be specified as "If there are two structures close enough, and if their membrane domains are compatible, fuse them to form a single structure".

The goal of the present report is to show that the cartoons used to represent Golgi trafficking can be translated into ABM models that produce quantitative predictions about Golgi stability and the transport of soluble and membrane-associated cargoes.

Results

Brief description of an ABM model for intracellular transport

In the ABM model for intracellular transport developed previously, organelles are membrane-bound structures, characterized by volume, area, and movement. The area of the organelles corresponds to the surrounding surface and it is covered by one or more membrane domains. The movement is determined by position, speed, and direction in a 2D space. Other agents included are microtubules. In ABM, each agent is interrogated about performing or not "actions", according to its specific situation. After all agents have performed or not the actions, the process is iterated with the new situation of the agents. In ABM, each iteration is called a "tick" and it is a variable that can be calibrated to represent physical time. For Golgi transport, the actions implemented where "movement", "fusion", "fission", "maturation", "influx", and "outflux". The frequency of each action can be specified by "ticks" (for example, do "maturation" every 3000 ticks) or assigning a probability assuming a Poisson distribution. Actions with higher probability occur more frequently than action with low probability (Table 1).

The space represented is a projection in 2D of a cytosol square of 4.5 x 4.5 μm. The relatively static position of the Golgi apparatus was mimicked by restricting the movement of cisternae to a perinuclear position and making vesicles to move towards the nucleus when near microtubules. These rules force the entire set of organelles to interact actively. For simplicity, other mechanisms that are likely involved in the recruitment of vesicles in the proximity of Golgi cisternae, such as tethering factors (Witkos and Lowe, 2017) were not considered in the models.

Vesicles and cisternae sensed all other structures at a distance less than its size (the radius of a sphere with the organelle's volume). When in contact, the fusion probability depended on the compatibility of the membrane domains of the two interacting organelles. During fission, a vesicle or cisterna was formed carrying a single membrane domain. Fusion and fission preserved the area, volume, and membrane domains of the organelles. In contrast, during maturation, all the membrane domains of an organelle were switched to (mature to) a single domain.

During influx, a new membrane domain was incorporated into the system by adding a new vesicle or cisterna, or by incorporating the domain to an existing cisterna. During outflux, a vesicle or cisterna was deleted from the model. The contents of the deleted organelle were summed to account for the transfer to a post-Golgi compartment.

Within these organelles, which dynamically change with time, soluble and membrane-associated cargo were included. The final destination of a cargo depended on its behavior during fission. Soluble cargoes were distributed according to the volume, and membrane-bound cargoes according to the area of the dividing organelles. Some cargoes had affinity for a membrane domain, and during fission, they followed the distribution of this domain. Large cargoes could not be included in newly formed vesicles and were retained in large cisternae.

Maturation model

In its simplest formulation, the Maturation model proposes that new cisternae are assembled in the cis side of the Golgi and that they mature to medial and trans cisternae with time. Finally, the cisternae leave the Golgi to become Trans Golgi Network (TGN) structures. To retain Golgi-resident factors (such as glycosyltransferases), these proteins are recruited in vesicles that fuse with the upcoming cisterna and they become engaged in a cycle of maturation and retrograde transport. These features of the model are represented in the schematic drawing shown in Figure 1A (modified from Alberts et al., 2015). According to this representation of Golgi transport, the process can be described by the following rules:

- New cisternae are formed in the cis side of the Golgi and are converted into TGN structures in the trans side of the organelle.
- The cisternae mature from cis to trans.
- Vesicles are formed in the cisternae carrying Golgi resident molecules and fuse to the previous cisterna to prevent the transport to the TGN.
- Vesicles are not allowed to fuse among them.
- Cisternae are not allowed to fuse among them.

To implement these rules in the ABM model, five "agents" with the characteristics of cisternae (500 nm in radius, 20 nm height cylinders) were generated, each one carrying a different membrane domain (C1 to C5). The cisternae could bud vesicles (fission) with the area and volume of a Cop I-type of structure (35 nm radius spheres). The vesicles could fuse with cisternae carrying a membrane domain corresponding to the previous cisterna in the cis-to-trans direction. For example, vesicles forming from C4 fused with the C3 cisterna (see fusion probability, Table 2). Vesicles forming from the C1 cisterna were deleted (they were supposed to leave the Golgi to fuse with ER/ERGIC structures). Every 3000 ticks, a new C1 cisterna was added. Simultaneously, the pre-existing

cisternae matured. This means that the old C1 cisterna switched to C2, C2 to C3, and so on. The C5 cisterna disappeared and the content was delivered to a post-Golgi compartment (TGN). Two snapshots of one simulation are shown in Figure 1B and the complete movie is included as supplemental material (Supplementary Movie 1).

Vesicular transport model

Vesicular Transport states that cargoes coming from the ERGIC are transported by vesicles that are formed in the different Golgi cisternae and fuse with the following one in the cis-to-trans direction. Conversely, another set of vesicles move in the trans-to-cis direction carrying backward cargoes. This simple description is captured in the cartoon shown in Figure 1C, which is a modification of the one shown in (Alberts et al., 2015). According to this representation of the Golgi transport, the process can be described by the following rules:

- All cisternae form two different types of vesicles.
- Forward (FW) vesicles bud from one cisterna and can only fuse with the following cisterna in the cis-to-trans direction.
- Backward (BW) vesicles bud from one cisterna and can only fuse with the following cisterna in the trans-to-cis direction.
- Forward vesicles carry cargoes that move forward in the secretory pathway.
- Backward vesicles are empty or carry cargoes moving backward in the secretory pathway.
- Vesicles are not allowed to fuse among them.
- Cisternae are not allowed to fuse among them.

To implement these rules in the ABM model, five cisternae carrying the C1 to C5 domains were generated. Since no maturation was allowed, the total area of each membrane domain remained constant during simulations, unless they were transported out of the Golgi. The cisternae could form 35 nm radius vesicles of two different kinds (FW and BW). The FW vesicles could only fuse with the following cisterna (e.g., FW C2 vesicles fuse with C3 cisternae), whereas the BW vesicles could only fuse with the previous cisterna (e.g., BW C2 vesicles fuse with C1 cisternae; see fusion probability Table 2). BW vesicles forming from the C1 cisterna were deleted (they leave the Golgi to fuse with ER/ERGIC elements). FW vesicles forming from the C5 cisterna were also deleted since they fuse with the TGN. Two snapshots of one simulation are shown in Figure 1D and the complete movie is included as supplemental material (Supplementary Movie 2)

Iterative fractionation (Distillation) model

In a seminal paper introducing the concept of iterative fractionation Frederick Maxfield wrote "… sorting may be accomplished in a more continuous fashion by many iterations of a sorting step. The

sorting step need not be particularly efficient since, like a fractional distillation apparatus, high efficiency sorting would result from repetition of the sorting step." (Dunn et al., 1989).

The idea was initially postulated for the endocytic route as a way to account for the efficient transport of ligands to lysosomes, and receptor sorting and recycling to the plasma membrane. However, the mechanism is general enough to be applied to any transport. In brief, fusion among organelles carrying compatible membrane domains promotes the mixing of compartments whereas fission causes the separation of membrane domains preserving the identity of the compartments. Cargoes in the interior of these organelles have then the possibility of interacting with different membrane domains and during fission, they are sorted according to the affinity for these membrane structures. Cargos without any affinity for membrane domains, are distributed homogeneously in the new organelles formed by fission. This model adapted to the Golgi structure is represented in the cartoon of Figure 1E and can be described by the following rules:

- All cisternae form a single type of vesicle carrying forward and backward cargoes.
- Vesicle budding from a cisterna can fuse with the same cisterna (homotypic fusion) or with the following or preceding cisternae (heterotypic fusion).
- Vesicles are not allowed to fuse among them.
- Only cisternae carrying the same predominant membrane domain can fuse.

To implement these rules in the ABM model, the same five cisternae carrying the C1 to C5 domains were generated. In this model also the total area of each membrane domain remained constant during simulations, unless they were transported out of the Golgi. The cisternae could form 35 nm radius vesicles surrounded by C1-C5 domains. The vesicles could fuse according to the fusion compatibility shown in Table 2 (high probability of fusing with its own cisterna, lower probability of fusing with the preceding or following cisterna, and null probability of fusion with other cisternae). Vesicles forming from the C1 cisterna were deleted randomly (mimicking the fusion with ER/ERGIC elements). Structures carrying C5 could also be deleted mimicking transport to the TGN. The probability of being selected for deletion was inversely proportional to the area of the C5 structure (large C5 organelles have less probability of being deleted). Membrane domains, volume, and area of the cisternae and vesicles were preserved during the fusion and fission steps. Two snapshots of one simulation are shown in Figure 1F and the complete movie is included as supplemental material (Supplementary Movie 3).

In summary, three models were implemented in Repast from drawings representing the Maturation, Vesicular, and Distillation transport hypotheses. We then run simulations to assess the stability and cargo transport capabilities of the models.

Stability of the models

The rules for each model correspond to the qualitative logic underlying the graphical representation for the different transport mechanisms. However, when implemented, the simulations show that they do not always generate a stable, well-organized Golgi apparatus. As parameters of the Golgi stability, the relative cisterna area for each Golgi domain was plotted throughout the simulations. An even distribution of areas would indicate a well-balanced Golgi. This distribution would have a maximal Shannon entropy (each domain occupying 20% of the total cisterna area renders an inter-cisternae entropy = 1.6). Also, in ideal conditions, individual organelles would carry a single Golgi domain; this distribution would render a minimal internal entropy (for example, if 100% of the area of a cisterna is a C1 domain, its intra-cisterna entropy is 0). To assess the performance of the different Golgi models, the cisternae relative area and the inter-cisternae and intra-cisterna entropies were plotted throughout the simulations (see Material and Methods for more details). The consistency of the results is shown in Supplemental Figure 1 where two single and a 10-simulation average are plotted.

Stability of the Maturation model

The progression of this model showed an unstable Golgi, with the five cisternae not present at all times (an artifact caused by the strict coordination between the influx and outflux of cisternae; result not shown). To stabilize the Golgi, a simple solution was to duplicate the C1 initial cisterna. With this setting, the duplicated area of the C1 cisterna disappear after a few fluctuations rendering a stable Golgi with high inter- and low intra- cisterna entropies (Figure 2A and 2B, middle panels). A clear periodicity was evident, dictated by the maturation process.

The stability of this Golgi model depends on the balance between the maturation and the rate of vesicle budding. In Figure 2A and 2B, vesicle budding probabilities (vb-p) of 0.002, 0.01 and 0.1 are shown. At a high budding rate (vb-p= 0.1), the Golgi became vesiculated and disorganized (Figure 2A and 2B, bottom panels). Notice the fluctuations of the individual cisterna areas causing a strong decrease of the inter-cisternae entropy. Also, the large number of vesicles promotes the mixing of membrane domains within a single cisterna, leading to a notorious intra-cisterna entropy increase. Single and average simulations are shown for stable (vb-p = 0.01) and unstable (vb-p = 0.1) Golgi in Supplementary Figure 1 (top panels).

Stability of the Vesicular model

Simulations with this model showed that the Golgi rapidly lost the C1 and C5 cisternae (not shown). Clearly, the model required the incorporation of these domains coming from the TGN and ERGIC as depicted in the cartoon as vesicles moving toward the cis and trans cisternae (Figure 1C). To implement this, a decrease of the C1 (or C5) area triggered the incorporation of the equivalent of a vesicle with a C1 (or C5) membrane domains to the C1 (or C5) cisterna. With this inward flux of membrane compensating the outward flux, the five cisternae were maintained.

However, the parameters for the Golgi stability were not as good as for the maturation model. The five cisternae were not always present and there was a mixture of domains in each cisterna (reflected in low inter-cisternae entropy and high intra-cisterna entropy, Figure 2C and 2D, top panels). An improved Golgi structure was obtained by allowing homotypic fusion of vesicles with the corresponding cisterna. Notice the better distribution of the Golgi area among the five cisternae (high inter-cisternae entropy) and the decrease in the intra-cisterna entropy (indicating less mixing of domains in each cisterna) when the probability of homotypic fusion (hf-p) was increased from 0 to 0.5 or 1 (Fig. 2C and 2D). Single and average simulations are shown for stable (hf-p = 1) and unstable (hf-p = 0) Golgi in Supplementary Figure 1 (middle panels).

Stability of the Distillation model

Similar to the Vesicular model, Distillation required the incorporation of domains coming from the TGN and ERGIC. However, even with this membrane flux, the Golgi was unstable with a poor separation among cisternae (Figure 2E and 2F, top panels). The high flexibility for fusion between vesicles of different origin with a cisterna promotes the mixing of Golgi domains. In the iterative fractionation model, fission is important to maintain the separation among membrane domains. This was evident in the endocytic pathway simulations (Mayorga and Campoy, 2010); compartments maintained their identity by forming not only vesicles but also large tubules. Similarly, the Golgi recovered its structure when the budding of a membrane domain was not restricted to form a 35 nm vesicle and was extended to larger cisterna-like structures. Figure 2E and 2F show the Golgi stability when the probability of budding structures larger than a vesicle (cb-p) was increased from 0 to 0.1 or 0.5. Notice that better parameters were obtained with the 0.1 probability; beyond this value, the inter-cisternae entropy decreased (Figure 2E and 2F, bottom panels). Single and average simulations are shown for stable (cb-p = 0.1) and unstable (cb-p = 0) Golgi in Supplementary Figure 1 (bottom panels).

Cargo transport in the models

To assess the transport capability of the three Golgi models, two different cargoes were included in the C1 cistern at the beginning of the simulations: a large soluble cargo and a small soluble cargo. The large cargo could not enter into vesicles and it was retained in the cisternae. Instead, the small cargo was distributed during fission according to the volume of the two structures formed. To mimic a Golgi resident enzyme, a membrane-bound cargo was also included. This cargo had affinity for the C3 membrane domain. During fission, it was enriched in the compartment carrying the C3 domain.

To measure transport, the simulation calculated the amount of each cargo associated with the different Golgi domains (C1 to C5) and the amount exiting the system from C5 structures (mimicking the transport to the TGN).

To assess whether the transport depends on the initial conditions, a second wave of transport was set at tick 30000 (the newly formed C1 structures at this tick were loaded with cargoes). The transport consistency is shown in Supplemental Figure 2 where single and average of 10 simulations are plotted.

Transport in the Maturation model

As expected for the maturation mechanism, the large cargo was transported at the rate of cisterna switching from C1 to C5 (Figure 3A, top panel). In contrast, the small soluble cargo, which could diffuse into all vesicles, was delayed in the Golgi and exited with kinetics approaching an exponential decay (Figure 3B, top panel). This was more evident when the vesicle budding rate was high (Supplementary Figure 2B, top left panel). The Golgi-resident enzyme could not enter into vesicles except in the C3 cisternae where it was recruited into the C3-formed vesicles (this would mimic the retrograde transport of a medial Golgi resident enzyme). This cargo was efficiently retrieved from the C3 cisterna by vesicles and remained cycling between C2-C3 cisternae for extended periods of time (Figure 3C, top panel). Notice, however, that at low budding probability ($p = 0.002$), the Golgi resident enzyme could not be retrieved and was lost by maturation (Supplementary Figure 2B, top central panel). Also, when the amount loaded in the Golgi was large, the vesicle capacity for backward transport was saturated and the enzyme was transported out of the Golgi (Supplementary Figure 2B, top right panel).

The transport process was very robust and occurred efficiently even under conditions where the Golgi was not stabilized. There were no major differences between the transport after the first and the second cargo pulse (Figure 3A, 3B, and 3C, top panes). Most of the transport characteristics described for this model can be appreciated in Supplementary Movie 1.

Transport in the Vesicular model

When cargoes were included in C1, the large one (that cannot enter into vesicles) was not transported and remained in C1 (Figure 3A, middle panel), whereas the small cargo was efficiently transported from C1 to C5 and eventually left the Golgi (Figure 3B, middle panel). It is worth mentioning that the small cargo was distributed between cisternae and FW vesicles proportional to the volume of the structures. In contrast, it was not incorporated in BW vesicles. The transport rate of the cargo depended on the possibility of being packed in vesicles. A membrane-associated cargo that was preferentially recruited in FW vesicles was rapidly transported (Supplemental Figure 2B, middle left panel). A Golgi resident enzyme was modeled as a cargo with affinity for the C3 domain and it was efficiently retained in the C3 cisterna (Figure 3C middle panel). Decreasing the homotypic fusion probability (hfp-p = 0; Supplemental Figure 2B, middle central panel) or increasing the amount added in each pulse of this cargo (Supplemental Figure 2B, middle right panel) caused a

defect on the transport to the C3 cisterna. Most of the transport characteristics described for this model can be appreciated in Supplementary Movie 2.

Transport in the Distillation model

In this model, transport is bidirectional. Soluble cargoes with no affinity for Golgi domains were distributed according to the volume of the cisternae. The forward transport depended on the membrane flux generated by the disappearance of vesicles and cisternae at the trans side of the Golgi. Notice that the large soluble cargo moved back and forward until it was trapped in a C5 cisterna that eventually left the Golgi (Figure 3A, bottom panel). This cargo was not transported unless the budding of structures larger than a vesicle was allowed (cb-p = 0.1; Supplemental Figure 2B, bottom right panel). The small cargo found its way to C5 cisternae and left the Golgi with exponential kinetics (Figure 3B, bottom panel). Cargoes with affinity for a specific Golgi domain could travel forward or backward to find its target. A cargo with affinity for the C3 domain loaded in C1 or C4 was rapidly transported to the C3 cisterna and remain there for extended periods of time (Figure 3C, bottom panel and Supplemental Figure 2B, bottom central panel). The distribution of this cargo was resistant to a hundred increase of its concentration (Supplemental Figure 2B, bottom right panel). Most of the transport characteristics described for this model can be appreciated in Supplementary Movie 3.

Changing rules and mixing models

The models implemented are interpretations of very simplistic cartoons. In more realistic models, rules should represent molecular mechanisms. For example, the rule that forces the maturation of all domains in a cisterna would be appropriated only for a positional definition of the cisternae. In a more mechanistic model for maturation (for example, mediated by a Rab cascade, Rivera-Molina and Novick, 2009) individual membrane domains would undergo independent maturation within each cisterna. When this rule was applied, the Golgi was still stable, however, an increase in the intra-cistena entropy was observed (Figure 4, top panels). Transport of large and small cargoes was also efficient, and a Golgi-resident membrane molecule was retained in the corresponding cisterna (Figure 4, top panels). This observation suggests that more mechanistic rules can be applied to simulate the maturation of cisternae.

In the vesicular model, the rules that establish the presence of FW and BW vesicles would require a very large number of specific SNAREs and tethers to implement the directionality of the two sets of vesicles. In a simplified version, a single set of FW vesicles was allowed. Surprisingly, the Golgi structure was preserved. Homotypic fusion was sufficient to restore the membrane domains transported to the following cisterna to the original organelle. The stability was not as good as when BW vesicles were allowed. An alternation of C4/C5 cisternae was observed that caused a decrease of the inter-cisternae entropy (Figure 4, middle panels). Transport was slower (notice the change of the abscissa scale) but conserved the same characteristics: no transport of large and efficient transport of small and Golgi-resident membrane cargoes (Figure 4, middle panels). In conclusion,

homotypic fusion not only improves the stability of the Golgi but also can simplify the set of vesicles required for transport.

It is likely that the real mechanism for Golgi transport is a combination of the models proposed here and in the literature. As an example of this possibility, a model was implemented combining the flexibility of the vesicle fusion of the Distillation model with the regular flux and maturation of membranes postulated by the Maturation model. This mixed model had excellent stability (Figure 4, bottom panels). Notice that the cisterna budding probability (cb-p) that was required for the stability of the Distillation model could be relaxed from 0.1 to 0.01. Transport was efficient for all cargoes, preserving the fast kinetics for the small cargo observed in the Distillation model (Figure 4, bottom panels). These observations suggest that it should be important to think of Golgi transport as a blend of possibilities sharing the fundamental processes of fusion, fission, and maturation.

Simulating glycosylation in the Distillation model

Molecular interactions and chemical reactions can easily be implemented on top of the ABM model (Mei et al., 2014). Each agent can send its composition to the ODE-solving software COPASI that will calculate the molecular changes according to a series of differential equations. COPASI will return a time series with these changes that will be used to update the composition of the organelle. COPASI works with physical time and molecular units (moles or number of molecules); Repast with ticks, area units (for membrane-associated molecules), and volume units (for soluble molecules). The conversion we have applied is explained in Methods. Whenever an organelle changes due to an ABM action (e.g., fusion or fission), COPASI is called and a new time series is calculated.

As an example of this strategy, a set of cisternae containing three glycosylation enzymes (E1, E2, E3 with affinity for C1, C2, and C3 Golgi domains, respectively) were allowed to stabilize using the Distillation model for 30000 ticks (about 30 min, see Methods for this equivalence). Then, a membrane-bound substrate for these enzymes was loaded in a C1 cisterna at 0.01 mM concentration and the glycosylation of the substrate as it traveled through the Golgi was followed for another 30 min. A cartoon of the model is shown in Figure 5A. The reactions implemented in COPASI are listed in Table 3. Notice that the enzymes were conveniently localized to the cisternae as the cargoes were transported and glycosylated (Figure 5B bottom panels). The kinetics of the enzymes was adjusted to prevent that a significant amount of substrate left the Golgi only partially glycosylated (most of the molecules recovered in post-Golgi structures were fully glycosylated; Figure 5B, right panel on the middle). COPASI allows following the glycosylation reactions in all organelles. As an example, the glycosylation is shown in two vesicles and three cisternae after 200 ticks in Figure 5C.

Distillation was not particularly suitable to implement the set of reactions required for glycosylation. Any model where Golgi resident enzymes are retained in the cisternae while substrates are

transported would support glycosylation. Simulations for Maturation, Vesicular, and the mixed Distillation + Maturation models were performed and the results included as Supplementary Figure 3. Notice that for the Maturation model, the first enzyme was located in the C2 cisterna. As explained before, in this model vesicles forming from the C1 cisterna were deleted (they were supposed to leave the Golgi to fuse with ER/ERGIC structures). In the three models, the enzymes were retained in the Golgi as the substrate S was transported from C1 to the TGN. En route, it was glycosylated as it met the appropriate enzymes. Notice that the three models supported efficient glycosylation, although, as expected, the substrate transport kinetics to the TGN were different.

Discussion

Intracellular transport is a very dynamic process involving organelles that move actively, changing shape and composition, and that undergo dramatic rearrangements of membrane and soluble factors by fusion with other organelles and budding of tubules and vesicles. It is hard to put together all these events to formulate a hypothesis about the underlying logic of transport of lipids, proteins, and carbohydrates. However, for years it has been evident from a large set of experimental approaches that membrane and soluble factors of different nature find their ways into the labyrinth of intracellular compartments in a robust and predictable way. Moreover, hundreds of factors required for the process have been identified and their function carefully characterized; many of them have been related to human diseases (De Matteis and Luini, 2011).

Despite of all these data, the mechanisms are still not well understood. In books, reviews, and publications, compartments are depicted as static structures, and transport is represented by arrows, frequently missing the dynamic changes observed in real-time movies.

In this report, we want to stress the necessity of more realistic models that capture the essence of intracellular trafficking. We also want to provide a modeling strategy that is flexible enough to translate a schematic drawing into a functional simulation that is able to generate quantitative predictions.

As an example of the flexibility of this modeling strategy, we have simulated the maturation and vesicular hypotheses for Golgi transport in their more classical and simplistic versions (Alberts et al., 2015). We also modeled the iterative fractionation or distillation transport mechanism that we have previously used for the endocytic route, adapted to the characteristics of the Golgi apparatus (Mayorga and Campoy, 2010).

It is important to stress that the different models for Golgi transport share several common features. The three requires fusion of membrane-bound structures and fission of budding vesicles/cisternae. These two processes are key for intracellular trafficking. Another common feature is membrane flux. The Golgi apparatus is not a closed system and requires the influx and efflux of membrane-bound structures. This is especially evident for the maturation model, but it is also present in the vesicular transport and distillation models.

Maturation, at present the most widely accepted model, needs to postulate additional mechanisms to fit the experimental data. For example, the fact that albumin (and other small soluble proteins) travel through the Golgi faster than procollagen (a large cargo that cannot enter into vesicles) does not fit with the model. To account for these observations, dynamic connections among cisternae are postulated (Beznoussenko et al., 2014). These connections would permit the fast diffusion of small cargoes. On the other hand, vesicular transport also requires additional transport mechanisms. By itself, it cannot account for the efficient transport of large cargoes that cannot fit into vesicles. So, the compartment carrying these cargoes are postulated to change by sporadic heterotypic fusion with adjacent stacks that would allow the transport of large cargoes without leaving the cisternae (Lavieu et al., 2014). The iterative fractionation model has several attractive features. It applies to the endocytic and secretory pathways and it can be interpreted as a version of the maturation and vesicular transport models. In yeast, the switch of a cargo-containing Golgi compartment by the acquisition of a trans marker as the cis marker was leaving has been well documented (Kurokawa et al., 2019). In the report by Nakano's group, both markers were membrane proteins, so the switch could not be done by exchanging factors with the cytosol and required the incoming and outgoing of membrane-bound organelles, an observation that perfectly fits with the distillation model. In this model, vesicles are not only carriers for cargo molecules; they are also vehicles for the transfer of membrane domains, and hence they can actively participate in the switch of cisterna identity. Notice that as postulated by the maturation model, they carry Golgi resident molecules.

The distillation model has also some common features with vesicular transport assuming a single set of vesicles that transport not only cargoes but also Golgi domains. Soluble and membrane-associated molecules with no specific affinity would be transported by the flux of material that is added at the cis side of the Golgi and is withdrawn at the trans side. Forward or backward transport is dictated by the affinity of cargoes for different Golgi domains. The high efficiency of the distillation model is dictated by the iterative fractionation of cargoes among membrane domains. In fact, the Golgi stack has been compared to a distillation tower to explain the high fidelity sorting of secreted cargoes from ER-resident proteins (Miesenböck and Rothman, 1995; Rothman, 1981).

In this report, we show that the basic rules that support a hypothetical transport mechanism can be extracted from a schematic drawing, and that these rules are sufficient to build an ABM simulation rendering quantitative predictions. It is important to stress that each rule should have an underlying molecular mechanism that we have not explored. For example, the hypothesis that vesicles budding from a cisterna fuse only with the preceding (or the following) cisterna would require the

identification of factors involved in specific recognition and fusion, and the maintenance of these factors in the correct localization to be incorporated into vesicles for the next round of fusion. In this sense, the distillation model has a simple explanation for Golgi homeostasis. According to this model, the Golgi domains are stable structures budding vesicles that fuse predominantly in a homotypic way. Patches of membrane domains which do not correspond to a specific Golgi compartment will be incorporated into budding vesicles that will preferentially fuse homotypically, restoring the factors to their original compartment.

However, for more complete transport mechanisms, it should be considered that membrane domains may undergo maturation. A classic example is the Rab5/Rab7 switch in the endocytic pathway that triggers the maturation of early to late endosomes. Rab cascades have also been characterized in the secretory pathway (Rivera-Molina and Novick, 2009; Papanikou and Glick, 2014; Novick, 2016). COPASI can be used to program ODE-based Rab conversion cascades leading to membrane domains maturation (Mayorga et al., 2018). Rabs and many of their effectors are peripheral membrane proteins that can equilibrate with cytosolic pools. This cytosol/membrane interplay can be incorporated in models by adding a “cytosol” agent that exchange molecules with the organelles.

In fact, the communication between Repast and COPASI can be used to include, in the skeleton of dynamic organelles, complex networks of molecular interactions and chemical reactions. This makes the modeling suitable for many processes that heavily depends on intracellular trafficking, such as receptor signaling, antigen processing, and cellular infections. As a very naïve example, the glycosylation of a hypothetical factor by three different enzymes located to different cisternae of the Golgi was implemented in COPASI. In this simulation, glycosylation occurred in dynamic structures that continuously change composition as the glycosylated factor and the enzymes were transported through the Golgi.

It is clear that our approach is not the first mathematical model implemented to represent the Golgi structure and the transport of cargoes (Vagne and Sens, 2018a; Vagne and Sens, 2018b; Dmitrieff et al., 2013; Binder et al., 2009; Ispolatov and Musch, 2013; Mukherji and O'Shea, 2014; Sachdeva et al., 2016; Gong et al., 2010). Several research groups have published different models addressing organelle self-organization and protein and lipid sorting in the Golgi (Kuhnle et al., 2010; Sens and Rao, 2013; Vagne et al., 2020). Fusion, fission, and maturation are at the core of most of these models. They are based on physical principles with different degrees of mathematical complexity and most can be analytically solved. Our method in these respects has limitations. Its advantages are simplicity and flexibility that would be crucial for building more complex pathways incorporating organelles of different nature. It is also easier to connect with cell biologists’ hypotheses. The schematic drawings of compartments connected with arrows can be conveniently represented in ABM and the molecular interactions in ODE, providing multiscale support to the simulations. This modeling strategy can be used to address issues directly linked to the mechanism of transport (e.g.,

Rab dynamics) or as a way to incorporate the complexity of transport to other cellular processes that occur in dynamic organelles (e.g., antigen presentation or cell infection).

As any other modeling strategy, the one proposed here has shortcomings, for example: i) COPASI calculations assume a homogeneous distribution of the species, including membrane-associated molecules. ii) The scenario is a projection in two dimensions of the real 3D space. iii) The form of organelles depends only on their volume and area, which are not enough to represent the shape of real organelles. These and other limitations can be solved in more complex versions of the model. As written by Gunawardena "…formal models are not descriptions of reality; they are descriptions of our assumptions about reality; they are only as good as their assumptions…" (Gunawardena, 2014).

All considering, the goal of this report was to show that dynamic models can be built extracting the rules implicitly present in Golgi transport cartoons. One motivation for having these models will be to distinguish between competing hypotheses. Improved imaging techniques and smart experimental tools (e.g. the RUSH system, Boncompain et al., 2012) to assess the dynamics of Golgi transport are presently available and they can be used to challenge the quantitative predictions of models that would not be self-evident from cartoons. The second motivation would be to include the dynamics of interacting compartments in the study of complex networks of protein interactions and chemical reactions occurring in the cell. At present, rules need to be programmed in Java; we have not generated a complete set of rules to choose from. We offer to help in the building of any model that interested groups may require. A long-term goal would be to make accessible more user-friendly tools to recreate a complete set of rules and to extend the model to embrace the endocytic and secretory pathways in a single simulation.

Materials and Methods

Agent-based model (Repast). The freely available modeling platform Repast (North et al., 2013) was used to model agents and actions in an Eclipse environment (https://repast.github.io/). The code can be accessed from the Git repository https://github.com/ihem-institute or from https://mega.nz/folder/pcpzwSKb#zl56zApweQgn1U4Ldyk8XA.

Ordinary differential equations (COPASI). ODEs were programmed in COPASI (Hoops et al., 2006)(http://COPASI.org/). All COPASI files are included in the Git repository. COPASI and Repast interaction is achieved as described before (Mei et al., 2014). Basically, Repast sends initial concentrations present in each organelle to COPASI that generates a time series. A matrix with time series for each metabolite is sent back to Repast.

World. The space represented is a projection in 2D of a cytosol square of 4.5 x 4.5 μm. The upper border corresponds to the plasma membrane and the lower border to the nucleus. The right and left borders form a continuous. Hence, the world shape corresponds to the surface of a cylinder.

Time. The tick duration was calibrated with the fastest process in the model (movement of organelles on microtubules: 1 μm/sec). In the simulation, an agent requires 75 ticks to travel 4.5 μm when associated with a microtubule; hence, one tick corresponds to about 0.06 sec. The frequency for all other actions was adjusted assuming Poisson distributions. Actions occurred every 0.06 seconds with the probabilities shown in Table 1.

Cisternae and vesicles. Each Golgi structure (cisterna or vesicle) has area and volume. The area is occupied by one or more of five Golgi domains (C1 to C5). The structures also carry membrane and soluble cargoes. In Repast, soluble cargoes were expressed as a fraction of the organelle volume, and membrane-associated cargo as a fraction of the organelle area. We assumed that these fractions roughly correspond to concentrations in mM units. According to this assumption, about 20 molecules of a soluble cargo at 1 mM concentration will be present in a 20 nm radius vesicle. This value fits well with the reported range of membrane proteins in an average synaptic vesicle of 21 nm radius (2-70 molecules, Takamori et al., 2006). The cargoes were loaded at 0.004 or 0.4 area or volume ration (corresponding to 0.004 or 0.4 mM, respectively). The transport capacity of an organelle of soluble or membrane cargoes was limited to 1 mM. No cargo was allowed to exceed this concentration making transport a saturable process.

The shape and size of cisternae correspond to 20 nm high cylinders with the area and volume of the cisterna. The cylinders were represented as round-corner rectangles in the 2D representation of the world. Vesicles are 35 nm radius spheres and are shown as circles. Cisternae and vesicles can perform the following actions:

Move. When near microtubules (light blue straight lines in the model), vesicles and small cisternae move to the minus end of the filament (toward the nucleus). Otherwise, they move randomly. Large cisternae (>250 nm radius) had fixed positions parallel to the nucleus and centered on the World (snapshots in Figure 1B, 1D, 1F, and 5C).

Fusion. Vesicles and cisternae sensed all other structures at a distance less than its size (the radius of a sphere with the organelle's volume). If nearby structures carry a compatible membrane domain, they fuse. Compatibility was calculated as previously described (Mayorga and Campoy, 2010). The probability of fusion of single domain structures is specified in Table 2 for the different models. For structures carrying more than one domain, the probability was adjusted according to the proportional area occupied by each membrane domain. After fusion, a single organelle was formed carrying the area and volume and all the membrane and soluble components of the original structures.

Fission. Cisternae had the possibility of budding vesicles/cisternae. Fission always generates vesicles/cisternae carrying a single membrane domain. The domain that was incorporated in the new organelle was selected at random. The probability of budding vesicles/cisternae was proportional to the area of the cisterna. The probability was set to p = (organelle area – area of a 250 nm radius cisterna)/ (area of a 500 nm radius cisterna– area of a 250 nm radius cisterna). Soluble contents were distributed proportionally to the volume of the formed structures and membrane cargoes to the area of the two new organelles except when they have affinity for specific Golgi domains. In this case, they were directed to the new structure if they have more affinity for the Golgi domain forming the vesicle/cisterna than for the Golgi domains remaining in the cisterna. Large cargoes could not enter into vesicles and remain always in the cisternae. Soluble and membrane-bound cargoes occupied volume and area of the structures; hence, the budding structures carried, at most, the cargoes corresponding to the vesicle/cisterna volume or area. The area, volume, membrane, and soluble contents were preserved during fusion and fission events. Golgi domains were also maintained, except during Maturation (see specifications for this action).

Maturation. Every 3000 ticks, all domains in a cisterna mature to the domain of the following cisterna (e.g., a cisterna carrying 80% C2 and 20% C3 will mature to a cisterna carrying 100% C3). Alternatively, all domains in a cisterna mature to the following domain (e.g., a cisterna carrying 80% C2 and 20% C3, will mature to a cisterna carrying 80% C3 and 20% C4).

Outflux. C1 or C5 vesicles and cisternae had the possibility of leaving the system and were deleted. For maturation transport, the C5 cisterna left the Golgi every 3000 ticks; for vesicular transport, only C5 vesicles carrying cargo were transported out of the Golgi; for distillation, C5 structures were selected at random to leave the system. Larger structures had a lower probability of being selected. The probability was set to p =1 - (structure area – area of a 35 nm radius vesicles)/ 0.8E6 nm. Where 0.8E6 nm is twice the area of a 250 nm radius cistern. The cargoes present in the C5 structures that left the Golgi along the simulation were considered transported to a post-Golgi compartment. Vesicles budding from the C1 cisterna could also leave the system. However, the cargoes in the C1 structures leaving the Golgi were re-located in a C1 cisterna (to prevent retrograde transport in order to measure only forward transport).

Influx. New Golgi structures were allowed to form to compensate for the domains that left the system. For maturation transport, a C1 cisterna was introduced every 3000 ticks; for vesicular and distillation transport, C1 and C5 vesicles were randomly added to the system.

Pulse of cargoes. Cargoes were loaded in the initial C1 cisterna. For distillation transport, when indicated, one cargo was loaded in the C4 cisterna to show backward transport. For a second pulse, the cargoes were loaded in the newly formed C1 vesicles/cisternae at ticks 30000.

Microtubules. Straight lines were drawn in the model representing microtubules. In the present model, these structures can only change position with a 0.0001 probability.

Cargo glycosylation. As an example of Repast-COPASI combination, the glycosylation of a factor by three different Golgi-resident enzymes was modeled in the Distillation transport mechanism. Three enzymes (E1, E2, and E3) with affinity for different Golgi domains (C2, C3, and C4 for Maturation, and C1, C2, C3 for the other models) were loaded in the model at 0.004 mM concentration. After 30000 ticks, they arrived at a quasi-stable distribution. Then, the factor was loaded in a C1 cisterna at 0.01 mM concentration and the changes in the glycosylated species and their distribution throughout the Golgi structures were recorded for additional 30000 ticks. In the simulation, each structure sent to COPASI its enzyme and substrate content in mM units, and received a time series with the evolution of the species along time. The series was re-calculated every time the composition of the organelle was changed by a transport event (e.g., fusion and fission). The reactions are shown in Table 3.

Model initialization. The parameters and initial organelle characteristics were loaded from a csv (comma-separated values) file generated from a spreadsheet. The COPASI file was included in the Eclipse environment to be called from Repast when needed.

Besides the graphical visualization, the model generates several output tables with data about the simulation.

Membrane and soluble cargo distribution. The simulation calculated the amount of each soluble and membrane cargoes associated with the different Golgi domains. For example, to estimate the association of a soluble cargo with the C5 domains, the amount of cargo present in each endosome was multiplied by its relative content of C5 on the organelle (cargo content * C5 area/total area) and

added to a total. As a rule, the simulations were run several times and the values plotted in the figures are the average of 3-10 runs.

Relative area and entropies. To calculate the relative area and inter-cisternae entropy, all the cisternae of the simulation, larger than 250 nm radius, were classified according to their prevalent Golgi domain. The area of all cisternae carrying the same Golgi domain was summed and expressed as a proportion of the total cisternae area. The Shannon's entropy for this distribution was calculated as $-\Sigma\ p * \ln(p)$, where p is the proportion of each Golgi domain. To calculate the intra-cisterna entropy, the same calculation was done for the proportions of Golgi domain areas in every single organelle in the simulation. The global intra-cisterna entropy was calculated as the area-weighted average of the organelles' values.

Online supplementary material. Representative movies of the Maturation, Vesicular, and Distillation models are included as supplemental material. The edge color of the organelles indicates the more abundant Golgi domain in each structure. Edge color code is the same as in the Figures (C1=blue; C2=cyan; C3=green; C4=red; C5=yellow). The content color indicates the presence of cargoes (small = green; large = red; membrane-associated with affinity for C3 = blue).

Reference List

Alberts,B., Johnson,A., Lewis,J., Morgan,D., Raff,M., Roberts,K., and Walter,P. (2015). Molecular Biology of the Cell, Garland Science, Taylor & Francis Group, New York.

Beznoussenko, G.V., Parashuraman, S., Rizzo, R., Polishchuk, R., Martella, O., Di, G.D., Fusella, A., Spaar, A., Sallese, M., Capestrano, M.G., Pavelka, M., Vos, M.R., Rikers, Y.G., Helms, V., Mironov, A.A., and Luini, A. (2014) Transport of soluble proteins through the Golgi occurs by diffusion via continuities across cisternae. Elife. ***3***, 10.7554/eLife.02009

Binder, B., Goede, A., Berndt, N., and Holzhutter, H.G. (2009) A conceptual mathematical model of the dynamic self-organisation of distinct cellular organelles. PLoS. ONE. ***4***, e8295

Boncompain, G., Divoux, S., Gareil, N., de, F.H., Lescure, A., Latreche, L., Mercanti, V., Jollivet, F., Raposo, G., and Perez, F. (2012) Synchronization of secretory protein traffic in populations of cells. Nat. Methods. ***9***, 493-498

Bonifacino, J.S. and Glick, B.S. (2004) The mechanisms of vesicle budding and fusion. Cell ***116***, 153-166

De Matteis, M.A. and Luini, A. (2011) Mendelian disorders of membrane trafficking. N. Engl. J. Med. ***365***, 927-938

Dmitrieff, S., Rao, M., and Sens, P. (2013) Quantitative analysis of intra-Golgi transport shows intercisternal exchange for all cargo. Proc. Natl. Acad. Sci. U. S. A. ***110***, 15692-15697

Dunn, K.W., McGraw, T.E., and Maxfield, F.R. (1989) Iterative fractionation of recycling receptors from lysosomally destined ligands in an early sorting endosome. J. Cell Biol. ***109***, 3303-3314

Glick, B.S. and Luini, A. (2011) Models for Golgi traffic: a critical assessment. Cold Spring Harb. Perspect. Biol. ***3***, a005215

Gong, H., Guo, Y., Linstedt, A., and Schwartz, R. (2010) Discrete, continuous, and stochastic models of protein sorting in the Golgi apparatus. Phys. Rev. E. Stat. Nonlin. Soft. Matter Phys. ***81***, 011914

Gunawardena, J. (2014) Beware the tail that wags the dog: informal and formal models in biology. Mol. Biol. Cell. ***25***, 3441-3444

Hoops, S., Sahle, S., Gauges, R., Lee, C., Pahle, J., Simus, N., Singhal, M., Xu, L., Mendes, P., and Kummer, U. (2006) COPASI--a COmplex PAthway SImulator. Bioinformatics. ***22***, 3067-3074

Ispolatov, I. and Musch, A. (2013) A model for the self-organization of vesicular flux and protein distributions in the Golgi apparatus. PLoS. Comput. Biol. ***9***, e1003125

Jahn, R. and Fasshauer, D. (2012) Molecular machines governing exocytosis of synaptic vesicles. Nature. ***490***, 201-207

Kim, K. (2016) Cargo trafficking from the trans-Golgi network towards the endosome. Biol. Cell. ***108***, 205-218

Kuhnle, J., Shillcock, J., Mouritsen, O.G., and Weiss, M. (2010) A modeling approach to the self-assembly of the Golgi apparatus. Biophys. J. ***98***, 2839-2847

Kumar, A., Baycin-Hizal, D., Zhang, Y., Bowen, M.A., and Betenbaugh, M.J. (2015) Cellular traffic cops: the interplay between lipids and proteins regulates vesicular formation, trafficking, and signaling in mammalian cells. Curr. Opin. Biotechnol. ***36***, 215-221

Kurokawa, K., Osakada, H., Kojidani, T., Waga, M., Suda, Y., Asakawa, H., Haraguchi, T., and Nakano, A. (2019) Visualization of secretory cargo transport within the Golgi apparatus. J. Cell Biol. ***218***, 1602-1618

Lavieu, G., Dunlop, M.H., Lerich, A., Zheng, H., Bottanelli, F., and Rothman, J.E. (2014) The Golgi ribbon structure facilitates anterograde transport of large cargoes. Mol. Biol. Cell. ***25***, 3028-3036

Liu, L., Doray, B., and Kornfeld, S. (2018) Recycling of Golgi glycosyltransferases requires direct binding to coatomer. Proc. Natl. Acad. Sci. U. S. A. ***115***, 8984-8989

Luini, A. and Parashuraman, S. (2016). Golgi and TGN. In Encyclopedia of Cell Biology, volume 2, Organizational Cell Biology , (Bradshaw, R. A. and Stahl, P. D., eds). pp. 183-191, Elsevier, Academic Press, Oxford.

Mani, S. and Thattai, M. (2016) Stacking the odds for Golgi cisternal maturation. Elife. ***19***, e16231

Mayorga, L.S. and Campoy, E.M. (2010) Modeling fusion/fission-dependent intracellular transport of fluid phase markers. Traffic. ***11***, 1001-1015

Mayorga, L.S., Cebrian, I., Verma, M., Hoops, S., and Bassaganya-Riera, J. (2018) Reconstruction of endosomal organization and function by a combination of ODE and agent-based modeling strategies. Biology Direct ***13***, 25

McCullough, J., Colf, L.A., and Sundquist, W.I. (2013) Membrane fission reactions of the mammalian ESCRT pathway. Annu. Rev. Biochem. ***82***, 663-692

Mei, Y., Carbo, A., Hontecillas, R., Hoops, S., Liles, N., Lu, P., Philipson, C., and Bassaganya-Riera, J. (2014). ENISI MSM: A novel multi-scale modeling platform for computational immunology. In Bioinformatics and Biomedicine (BIBM). IEEE International Conference, pp. 391-396, IEEE.

Miaczynska, M. and Zerial, M. (2002) Mosaic organization of the endocytic pathway. Exp. Cell Res. ***272***, 8-14

Miesenböck, G. and Rothman, J.E. (1995) The capacity to retrieve escaped ER proteins extends to the trans-most cisterna of the Golgi stack. J. Cell Biol. ***129***, 309-319

Mukherji, S. and O'Shea, E.K. (2014) Mechanisms of organelle biogenesis govern stochastic fluctuations in organelle abundance. Elife. ***3***, e02678

North, M.J., Collier, N.T., Ozik, J., Tatara, E.R., Macal, C.M., Bragen, M., and Sydelko, P. (2013) Complex adaptive systems modeling with Repast Simphony. Complex Adaptive Systems Modeling ***1***, 3

Novick, P. (2016) Regulation of membrane traffic by Rab GEF and GAP cascades. Small GTPases. ***7***, 252-256

Papanikou, E. and Glick, B.S. (2014) Golgi compartmentation and identity. Curr. Opin. Cell Biol. ***29***, 74-81

Renard, H.F., Johannes, L., and Morsomme, P. (2018) Increasing Diversity of Biological Membrane Fission Mechanisms. Trends Cell Biol. ***28***, 274-286

Rivera-Molina, F.E. and Novick, P.J. (2009) A Rab GAP cascade defines the boundary between two Rab GTPases on the secretory pathway. Proc. Natl. Acad. Sci. U. S. A. ***106***, 14408-14413

Rothman, J.E. (1981) The golgi apparatus: two organelles in tandem. Science. ***213***, 1212-1219

Sachdeva, H., Barma, M., and Rao, M. (2016) Nonequilibrium description of de novo biogenesis and transport through Golgi-like cisternae. Sci. Rep. ***6***, 38840

Sens, P. and Rao, M. (2013) (Re)modeling the Golgi. Methods Cell Biol. ***118***, 299-310

Sudhof, T.C. and Rothman, J.E. (2009) Membrane fusion: grappling with SNARE and SM proteins. Science. ***323***, 474-477

Takamori, S., Holt, M., Stenius, K., Lemke, E.A., Gronborg, M., Riedel, D., Urlaub, H., Schenck, S., Brugger, B., Ringler, P., Muller, S.A., Rammner, B., Grater, F., Hub, J.S., De Groot, B.L., Mieskes, G., Moriyama, Y., Klingauf, J., Grubmuller, H., Heuser, J., Wieland, F., and Jahn, R. (2006) Molecular anatomy of a trafficking organelle. Cell. ***127***, 831-846

Vagne, Q. and Sens, P. (2018a) Stochastic Model of Maturation and Vesicular Exchange in Cellular Organelles. Biophys. J. ***114***, 947-957

Vagne, Q. and Sens, P. (2018b) Stochastic Model of Vesicular Sorting in Cellular Organelles. Phys. Rev. Lett. ***120***, 058102

Vagne, Q., Vrel, J.P., and Sens, P. (2020) A minimal self-organisation model of the Golgi apparatus. Elife. ***9***, e47318

Wickner, W. and Schekman, R. (2008) Membrane fusion. Nat. Struct. Mol. Biol. ***15***, 658-664

Witkos, T.M. and Lowe, M. (2017) Recognition and tethering of transport vesicles at the Golgi apparatus. Curr. Opin. Cell Biol. ***47***, 16-23

Table 1. Actions frequency for the different models. Frequency is expressed as a fixed number of ticks or as the probability of occurring in one tick

actions\models	Maturation	Vesicular	Distillation
move	1	1	1
fusion	0.001	0.006	0.006
fission	0.002, 0.01, or 0.1	0.12	0.5
influx	fixed (every 3000 ticks)	0.02	0.001
outflux	fixed (every 3000 ticks)	0.12	0.006
maturation	fixed (every 3000 ticks)	0	0

Table 2. Fusion probabilities between Golgi domains for the three transport models. Numbers are the fusion probability for any membrane domain present in a vesicle (column) to fuse with any membrane domain present in a cisterna (rows). The Vesicular model has two set of vesicles. Notice the asymmetric fusion probability for backward (BW, empty) and forward (FW, cargo carrying) vesicles. In this model, three different homotypic fusion probabilities were tested (0, 0.5, and 1).

Maturation					
cisterna \vesicle	C1	C2	C3	C4	C5
C1	0	1	0	0	0
C2	0	0	1	0	0
C3	0	0	0	1	0
C4	0	0	0	0	1
C5	0	0	0	0	0

Vesicular					
cisterna \vesicle	C1	C2	C3	C4	C5
C1	0, 0.5 or 1	BW 1 FW 0	0	0	0
C2	BW 0 FW 1	0, 0.5 or 1	BW 1 FW 0	0	0
C3	0	BW 0 FW 1	0, 0.5 or 1	BW 1 FW 0	0
C4	0	0	BW 0 FW 1	0, 0.5 or 1	BW 1 FW 0
C5	0	0	0	BW 0 FW 1	0, 0.5 or 1

Distillation					
cisterna \vesicle*	C1	C2	C3	C4	C5
C1	1	0.1	0	0	0
C2	0.1	1	0.1	0	0
C3	0	0.1	1	0.1	0
C4	0	0	0.1	1	0.1
C5	0	0	0	0.1	1

*two cisternae carrying the same domain could also fuse

Table 3. Set of irreversible reactions and kinetic functions programmed in COPASI. A substrate (S) is modified by three glycosidases (E1, E2, and E3) that incorporated three G residues. The concentration of G is maintained constant

Reaction's name	Reaction	kinetic function*
Gly1	S + G + E1 → S-G + E1	k1*[S]*[E1]
Gly2	S-G + G + E2 → S-GG + E2	k2*[S-G]*[E2]
Gly3	S-GG + G+ E3 → S-GGG + E3	k3*[S-GG]*[E3]

*Mass action kinetics (k1 = k2 = k3 = 125 µl/nmol/s)

Legends to the figures

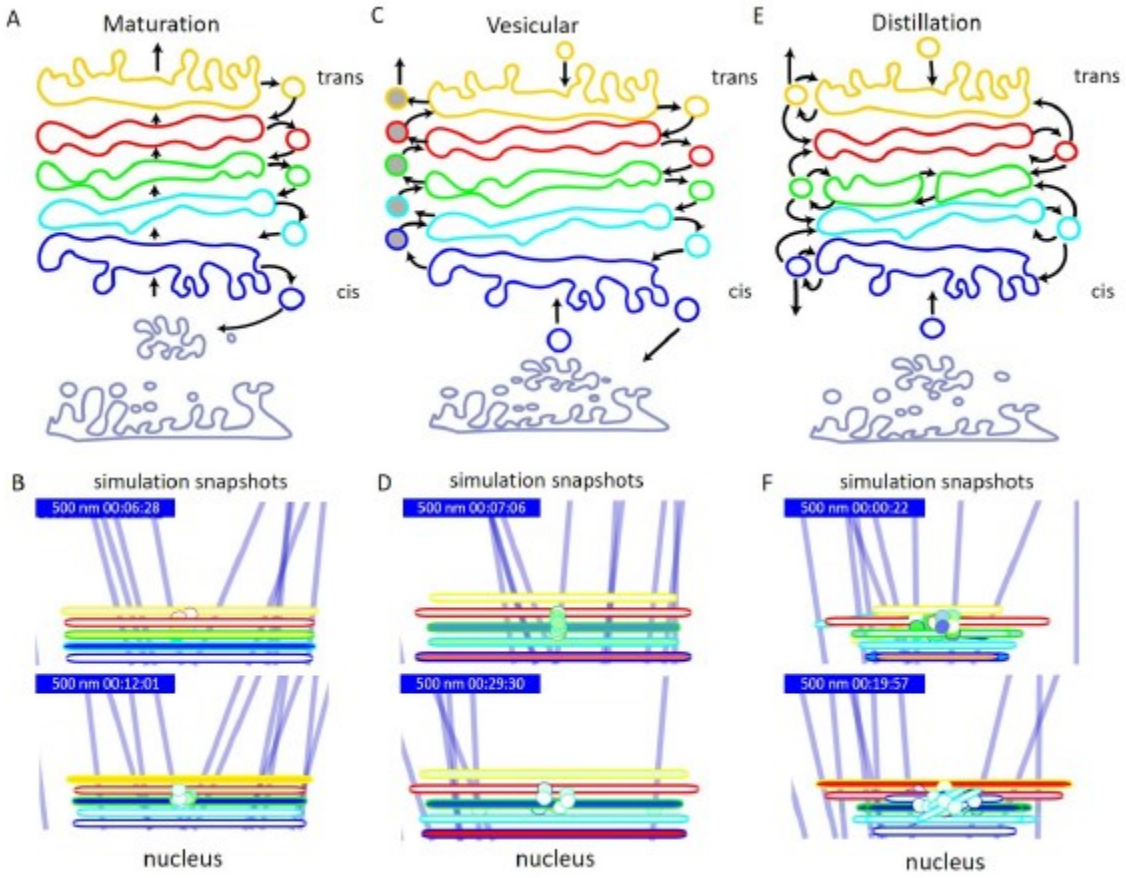

Figure 1. Golgi cartoons representing the Maturation, Vesicular, and Distillation models. (A) Cartoon representing the Maturation model. Notice the forward membrane flux/maturation process and the vesicle-mediated backward transport. (**B)** Two snapshots from Supplementary Movie 1 (example of a simulation built with Maturation rules). **(C)** Cartoon representing the Vesicular transport model. Notice that two types of vesicles can form from the cisternae. One type carries cargoes (gray lumen) and fuses only with the following cisterna in the cis-trans direction. The other type (white lumen) fuses with the previous cisterna. **(D)** Two snapshots from Supplementary Movie 2 (example of a simulation built with Vesicular rules). **(E)** Cartoon representing the Distillation model. Notice the possibility of undergoing homo and heterotypic fusion. Homotypic fusion among cisternae is also allowed. **(F)** Two snapshots from Supplementary Movie 3 (example of a simulation built with Distillation rules). For the snapshots, the edge color of the organelles indicates the more abundant Golgi domain in each structure (C1=blue; C2=cyan; C3=green; C4=red; C5=yellow). The content color indicates the presence of cargoes (small = green; large = red; membrane-associated with affinity for C3 = blue). Blue bars, 500 nm. See cargo description in Material and Methods. The simulation time is shown inside the bars (hh:mm:ss).

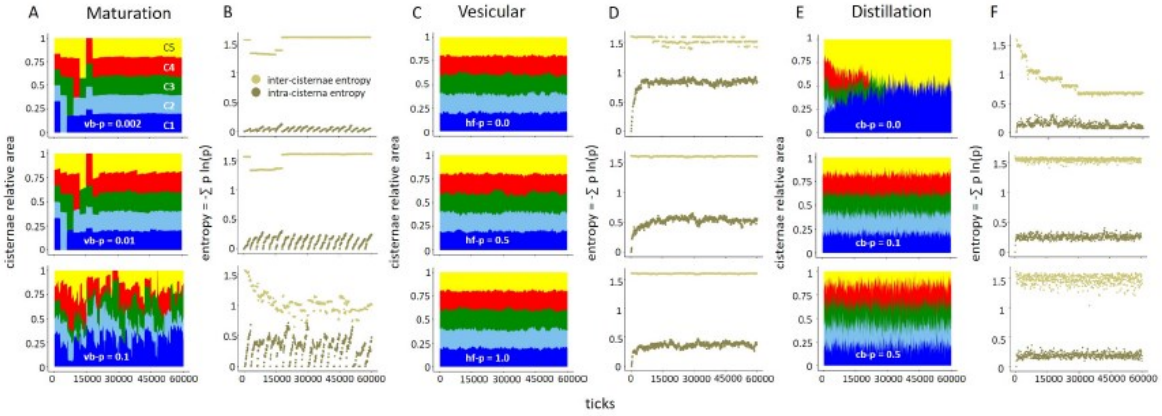

Figure 2. Golgi stability for the Maturation, Vesicular, and Distillation models. The stability is assessed by the distribution of the five Golgi domains used to build the organelle. An equilibrated "flag" pattern along the simulation (panels in A, C, and E) indicates a well-balanced Golgi with a high inter-cisternae entropy (light color spots, panels in B, D, and F). Mixing of Golgi domains in the same cisterna is measured by the intra-cisterna entropy (dark color spots, panels in B, D, and F), which should be low for a well-organized Golgi. The Maturation model was unstable when the vesicle budding probability (vb-p) was high (vb-p = 0.1, bottom panels in A and B). The Vesicular model presented inhomogeneous cisternae (large intra-cisterna entropy) when the probability of a vesicle to fuse homotypically with the corresponding cisterna (hf-p) was low (hf-p < 1, top and middle panels in C and D). The Distillation model was not well-organized when the probability of forming cisternae (cb-p) was null (cb-p = 0, top panels in E and F) or too high (cb-p = 0.5, bottom panels in E and F). The data in all panels represent the average of three simulations.

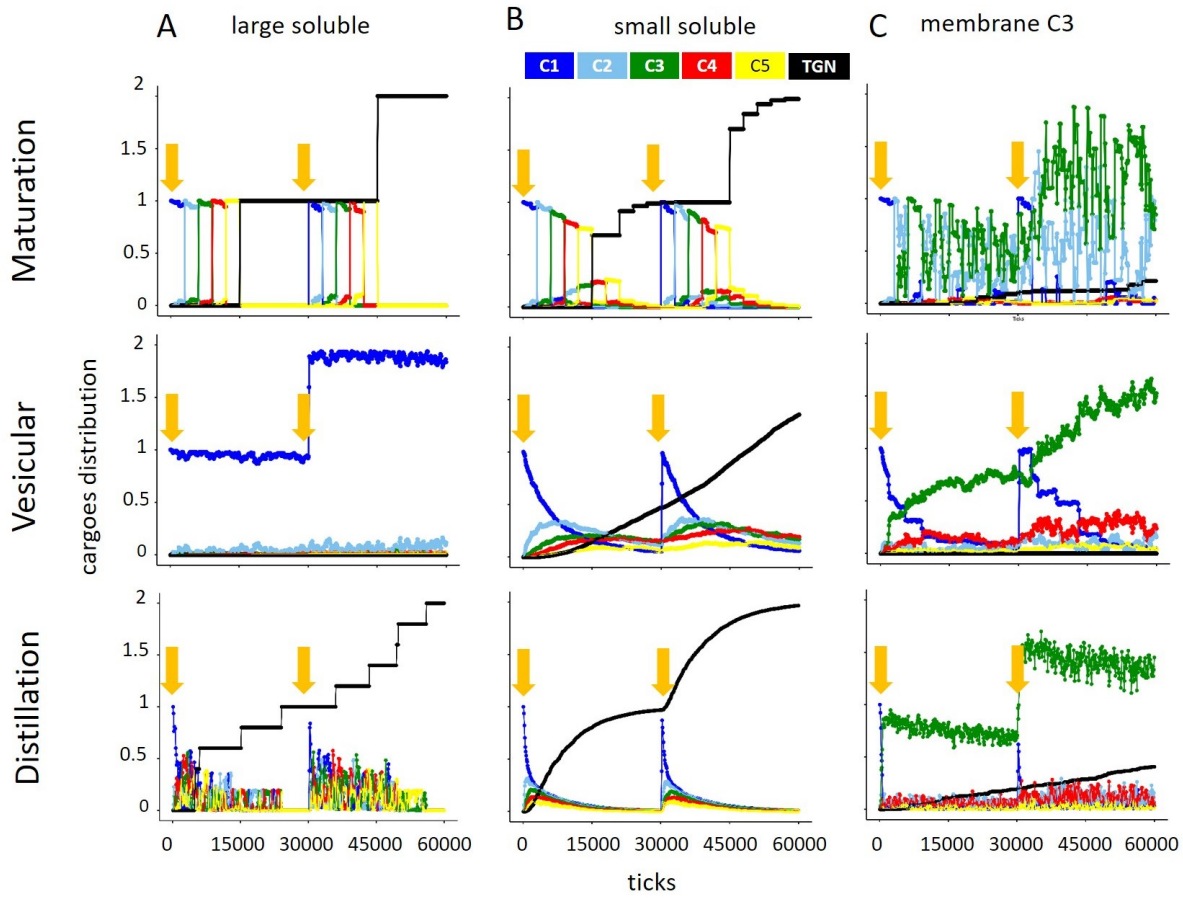

Figure 3. Cargoes transport in the Maturation, Vesicular, and Distillation Golgi models. The association of a large soluble (A), a small soluble (B), and a membrane-associated (C) cargo with the different Golgi domains (C1 to C5) or with post-Golgi compartment (TGN) was followed throughout the simulations. Stable Golgi conditions were used for the three models (vesicle budding probability = 0.01 for Maturation; homotypic vesicle-cisterna fusion probability = 1 for Vesicular; cisterna budding probability = 0.1 for Distillation). The large cargo could not fit into vesicles and was retained in cisternae. The small cargo was distributed during fission according to the volume of the two structures formed. The membrane-bound cargo had affinity for the C3 membrane domain. During fission, it was enriched in the compartment carrying the C3 domain. For the Maturation model, it was specifically recruited into C3 vesicles budding from the C3 cisterna. The cargoes were loaded in C1 cisternae at tick 0 and 30000 (arrows). The data in all panels represent the average of three simulations.

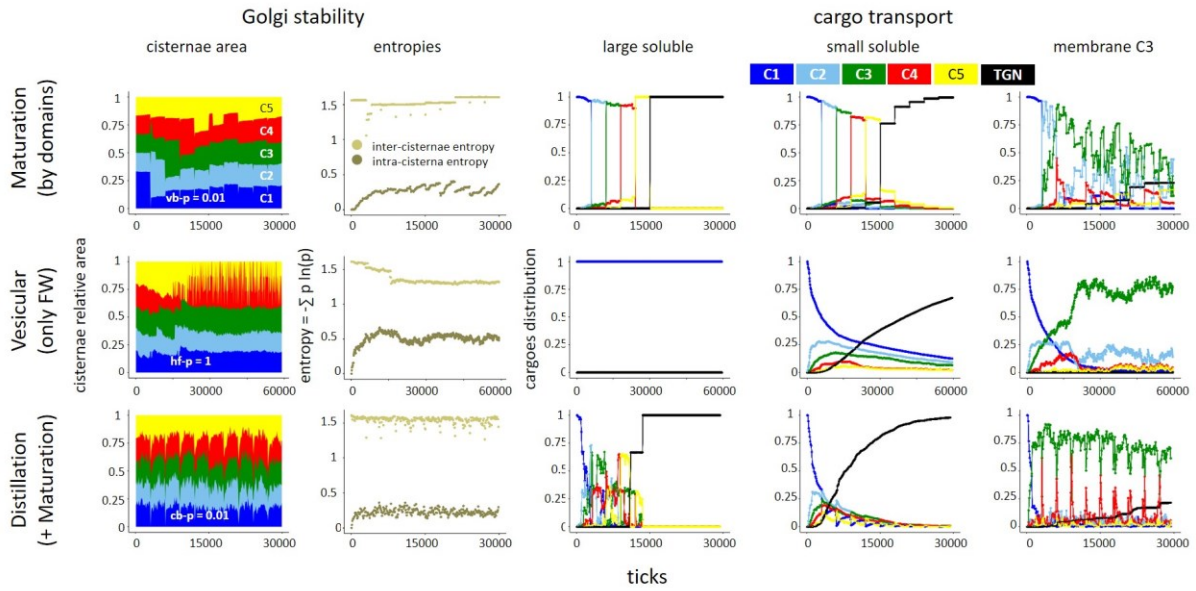

Figure 4. Golgi stability and cargo transport changing the rules and mixing the models. Top panels. Maturation model where the rule was changed: every 3000 ticks the domains in each cisterna switched to the next domain (C1 → C2 …. C4 → C5). **Middle panels.** Vesicular model where only FW vesicles were formed. **Bottom panels.** The flexible fusion rules of the Distillation model were combined with the membrane flux and cisternae maturation rules of the Maturation model. Golgi stability parameters (cisternae relative area and entropies) were calculated as explained in Figure 2. Cargo transport (cargo distribution) was expressed as explained in Figure 3. Notice the change in the abysses scale for the Vesicular model (middle panels). The data in all panels represent the average of three simulations.

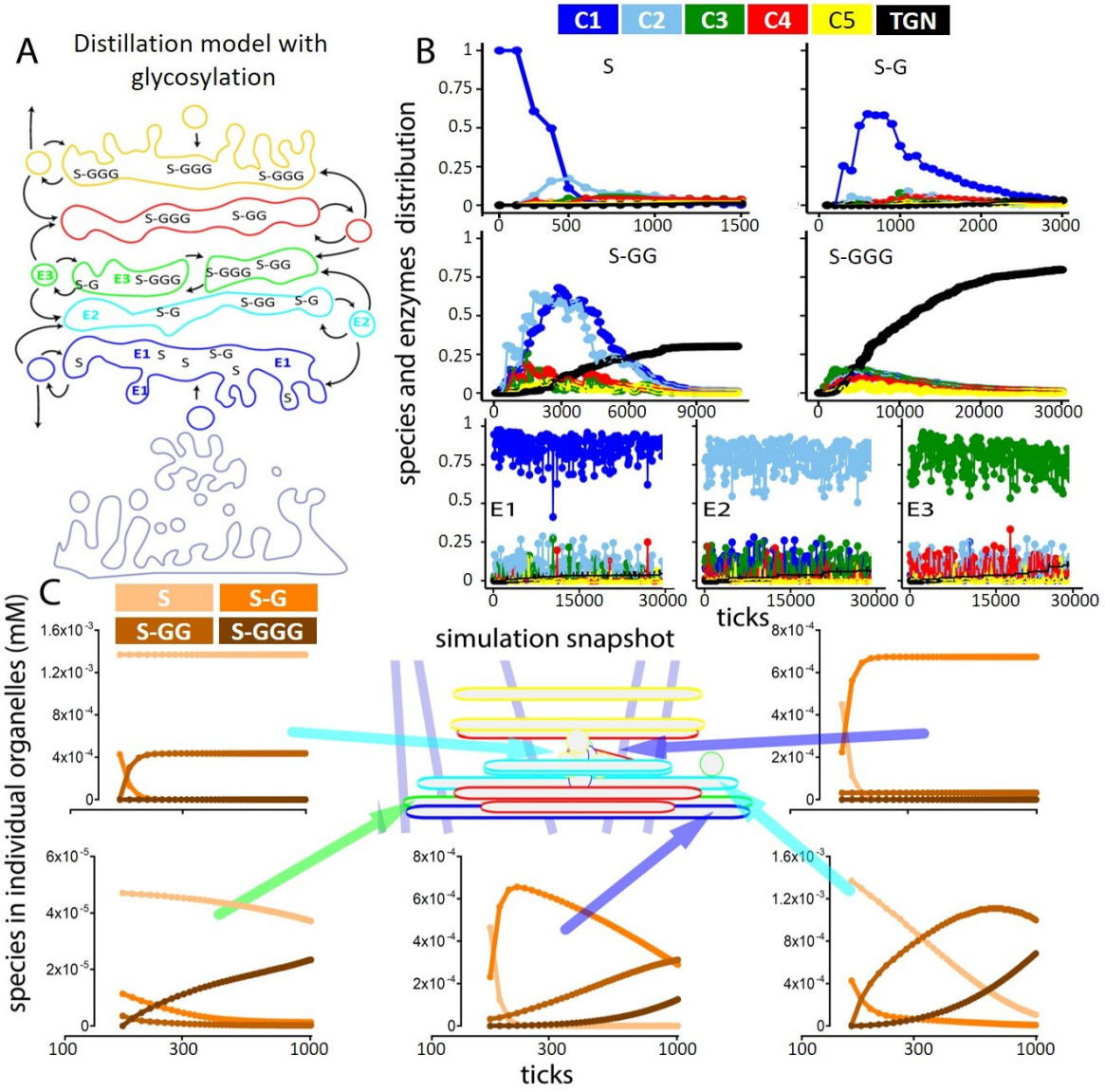

Figure 5. Glycosylation simulated within the Distillation model. **(A)** Cartoon representing the distillation model where a substrate is glycosylated by three enzymes (see reactions in Table 3). In the Distillation model, vesicles carry both cargoes and enzymes. **(B)** Transport of the non-glycosylated and glycosylated species (S, S-G, S-GG, and S-GGG), and three glycosyltransferases (E1, E2, and E3, with affinity for C1, C2, and C3 domains, respectively). The enzymes (0.004 mM) were equilibrated for 30000 ticks and then S was included in a C1 cisterna at 0.01 mM concentration. The association of the species and enzymes with the different Golgi domains or a post-Golgi compartment was followed throughout the simulation. The glycosylation process in each organelle was calculated by COPASI. In B, the results are normalized considering the maximal amount of cargo present in the simulation. **(C)** The simulation was stopped at tick 200 and the glycosylation time series calculated by COPASI for five individual organelles (two vesicles, top panels, and three cisternae, bottom panels) were plotted. The arrows point to the five organelles analyzed. The color of the arrows indicates the prevailing Golgi domain of the five organelles (blue, C1; cyan, C2; green, C3). For the snapshot in C, the edge color of the organelles indicates the more abundant Golgi domain in each structure (C1=blue; C2=cyan; C3=green; C4=red; C5=yellow).

Graphical Abstract

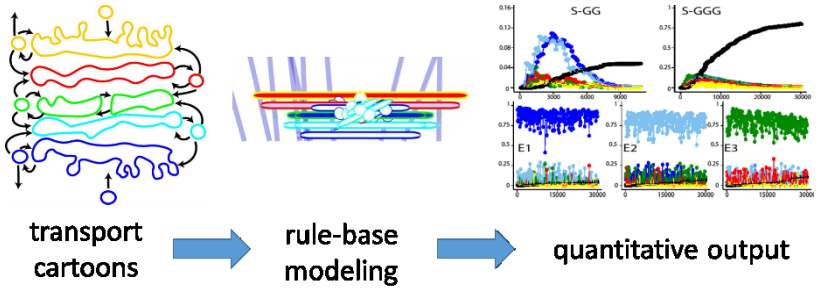

Schematic representations of Golgi trafficking can be easily translated into Agent-Based Models rendering quantitative predictions about Golgi stability and transport efficiency. The models can incorporate Ordinary Differential Equations to handle complex networks of molecular interactions and chemical reactions. The strategy described provides a simple, flexible, and multiscale tool to analyze Golgi transport and other cellular processes that occur in dynamic organelles.